# Randomly-Branched Polymers by Size Exclusion Chromatography with Triple Detection: Computer Simulation Study for Estimating Errors in the Distribution of Molar Mass and Branching Degree[a]

Luis A. Clementi, Jorge R. Vega, Gregorio R. Meira*

This article theoretically evaluates the biases introduced into the distributions of molar masses (MMD) and number of long chain branches per molecule (LCBD), when randomly-branched polymers are analyzed by size exclusion chromatography (SEC) with molar mass-sensitive detectors. The MMD of a polymer with tetrafunctional branch units is simulated under ideal SEC, i.e., θ-solvent, perfect measurements, and perfect fractionation by hydrodynamic volume except for a minor mixing in the detector cells. A negligible bias is introduced into the MMD, even when including band broadening in the columns. In contrast, poor MMD estimates are obtained when the chromatograms are contaminated with additive noise. Only qualitative estimates of the LCBD are possible.
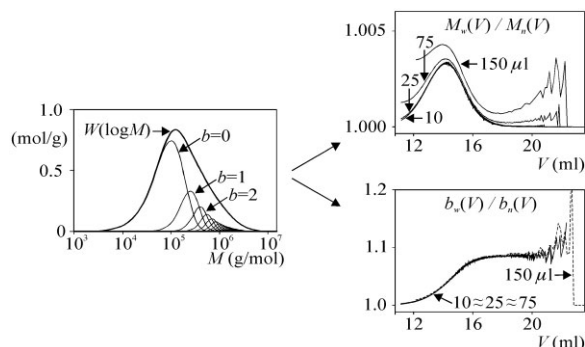
1. Introduction

Chain branching is present in many important polymers, both synthetic (such as polyacrylates), and natural (such as amylopectins). Short-chain branching affects the melting point, glass-transition temperature, hardness, and degree of crystallinity. Long-chain branching mainly affects rheological properties such as sedimentation behavior, intrinsic viscosity, and elongational viscosity of the polymer melt. Randomly-branched polymers are produced through chain- or step polymerizations involving monomers of functionality 3 or higher. Radical polymerizations of bifunctional monomers also generate random long branches (by intermolecular chain transfer to the polymer and/or by termination reactions), and random short branches (by intramolecular cyclization). Branched topologies are characterized by the number of branch units per molecule (or branching degree b), and by the functionality of the branch units (f). In star molecules, $b = 1$, and $f (= 3, 4, \ldots)$ is the number of arms.

Prof. L. A. Clementi, J. R. Vega
INTEC (Univ. Nac. del Litoral – CONICET), Güemes 3450 (3000),
Santa Fe, Argentina; and FRSF (Univ. Tec. Nacional), Lavaise 610
(3000), Santa Fe, Argentina
Prof. G. R. Meira
INTEC (Univ. Nac. del Litoral – CONICET), Güemes 3450 (3000),
Santa Fe, Argentina
E-mail: gmeira@santafe-conicet.gov.ar

[a]**Supporting Information** is available online from the Wiley Online Library or from the author.

Randomly-Branched Polymers by Size Exclusion Chromatography with Triple Detection . . .

Macromolecular
Theory and Simulations

www.mts-journal.de

In randomly-branched polymers, $b = 0, 1, 2, \ldots$, and f is typically $= 3$ or 4.

So far, no analytical technique is capable of fractionating molecules according to number of branches; and therefore no truly quantitative method is available for measuring the distribution of long chain branches per molecule (LCBD). For certain polymers, ^{13}C nuclear magnetic resonance spectroscopy (NMR) is an absolute technique for measuring average branching; and in the case of sparsely-branched polyolefins, branching frequencies as low as 0.001% of the total repeating units have been determined by melt-state, high-resolution, magic-angle spinning.[1] A further difficulty with ^{13}C NMR is that it cannot distinguish between short- and long chain branches.

Size exclusion chromatography (SEC) with triple detection [i.e.: fit with a differential refractometer (DR), a light-scattering detector at $0°$ (LS_0), and a specific viscometer (SV)] is presently the preferred (albeit indirect) technique for characterizing long chain branching.[2–8] In randomly-branched polymers, the branching degree increases with molar mass, and fractionation by hydrodynamic volume simultaneously provides some fractionation by branching degree. Linear molecules exhibit bigger hydrodynamic volumes than branched molecules of the same molar mass. For this reason, branched polymers are chromatographically complex, since even under perfect fractionation by hydrodynamic volume, whole distributions of molar masses and branching degrees are present in the detector cells. In practice, these local or instantaneous distributions are further broadened by imperfect resolution or band broadening (BB). For quantitative estimates of the MMD and LCBD, their local distributions must be narrow along the whole range of elution volumes.

The local average number of branches per molecule is indirectly estimated from the concept that a branched molecule is smaller than its linear homolog of the same molar mass. At a fixed molar mass (M), the geometric contraction factor is defined by:[9]

$$g \equiv \frac{R_{g,b}^2(M)}{R_{g,l}^2(M)} \leq 1; \quad (M = M_b = M_l) \tag{1}$$

Similarly, the viscometric contraction factor is defined by:[10]

$$g' \equiv \frac{[\eta]_b(M)}{[\eta]_l(M)} = \frac{[\eta]_b(M)}{k\,M^\alpha} \leq 1; \quad (M = M_b = M_l) \tag{2}$$

In Equation (1) and (2), the subscripts b and l indicate branched and linear molecules, respectively; R_g^2 is the average squared radius of gyration over all possible configurations and conformations; $[\eta]$ is the intrinsic viscosity; and (k, α) are the Mark–Houwink–Sakurada (MHS) constants of the linear homolog. Both contraction factors are interrelated through the semi-empirical expression:

$$g' = g^\varepsilon; \quad (0.5 \leq \varepsilon \leq 1.5) \tag{3}$$

where exponent ε is a measure of molecular drainability. For discussions and values of ε, see refs.[11–13] A further complication with Equation (3) is that ε is suspect of depending on molar mass.[14,15]

Direct determination of g via radii of gyration is in principle possible by multiangle LS/DR. However, this technique only provides accurate radii of gyration for $M > 10^5\,g\,mol^{-1}$.[8] In contrast, SV signals are somewhat more sensitive to low molar mass, enabling the determination of g' from measurements of $[\eta]_b(V)$. For linear Gaussian molecules dissolved in θ-solvents, Flory and Fox[16] developed the following expression for the radius of gyration:

$$R_{g,l}^3 = \frac{[\eta]_l\,M_l}{\Phi_l}, \quad (\Phi_l = \Phi_0 = 3.67 \times 10^{24}\,mol^{-1}) \tag{4}$$

Equation (4) has also been applied to star molecules of fixed functionality and varying M; and to randomly-branched polymers of fixed branching degrees and varying M.[17] In this last case, one can write:

$$R_{g,b}^3 = \frac{[\eta]_b\,M_b}{\Phi_b}; \quad (b = 1, 2, 3, \ldots); \quad (f = 3\,or\,4); \quad (\Phi_b > \Phi_l) \tag{5}$$

From Equation (1), (2), and (5), the following is obtained[17]:

$$g' = \frac{\Phi_b\,R_{g,b}^3}{\Phi_l\,R_{g,l}^3} = \frac{\Phi_b}{\Phi_l}\,g^{3/2}; \quad (M_b = M_l); \quad (b = 1, 2, 3, \ldots) \tag{6}$$

Finally, by introducing Equation (3) into Equation (6), one obtains:

$$\Phi_b = \frac{\Phi_l}{g^{3/2-\varepsilon}}; \quad (b = 1, 2, 3, \ldots) \tag{7}$$

With the assumptions: (i) intermolecular reactions are not considered, (ii) excluded volumes are neglected, and (iii) all functional groups have the same probability of reaction; Stockmayer[18,19] developed the following expression for the bivariate weight chain-length distribution of a randomly-branched polymer obtained by copolymerization of monomers of functionality 2 and $f \geq 3$:

$$w_{b,l} \propto (b+l)f\,\rho^{b-1}(1-\rho)^l\,p^{b+l-1}(1-p)^{fb-2b+2}$$
$$\times \frac{(f\,b-b+l)!}{b!\,l!\,(f\,b-2b+2)!} \quad (b = 0, 1, 2, \ldots); \quad (l = 1, 2, \ldots) \tag{8}$$

Materials
Views
www.MaterialsViews.com

Macromol. Theory Simul. **2014**, *23*, 90–100
© 2013 WILEY-VCH Verlag GmbH Co. KGaA, Weinheim

Macromolecular
Journals

91

where $w_{b,l}$ is the weight fraction of molecular species containing l bifunctional units and b f-functional units; p $(0 \leq p \leq 1)$ is the extent of reaction (or ratio between the number of reacted groups and the total initial number of reactive groups); and ρ is the recipe or initial ratio between the number of reactive groups contained in f-functional monomers and the total number of reactive groups.

For $f = 4$, Thurmond and Zimm[20] developed the following alternative recursive expression for Equation (8):

$$ w_{b,l} \propto \frac{\gamma(2/\bar{y}_w)^3 l^3}{2b(2b+1)(2b+2)} w_{b-1,l} \quad \text{with}: \quad w_{0,l} = \frac{2l}{\bar{y}_w} e^{-(2+\gamma)l/\bar{y}_w} $$

(9a)

and

$$ \bar{y}_w = \frac{2}{1-p}; \quad \gamma = \rho \bar{y}_w $$

(9b)

where b is the number of tetrafunctional branch units per molecule; $\bar{y}_w$ is the weight-average degree of polymerization of primary linear molecules (i.e.: molecules that would exist if all cross-links were severed); and γ (with $0 \leq \gamma \leq 1$) is the branching parameter that tends to unity at the gel point. To obtain a pregel of a moderately high number-average chain length and with most of its branch units linked onto f linear chains of bifunctional repetitive units, the following parameters are required: $p \approx 1$ and $\rho << 1$.

In SEC with triple detection, the branching functions $b_n(\log M)$ or $b_w(\log M)$ are typically calculated as follows.[21–23] First, $M_w(V)$ and $[\eta](V)$ are estimated from the signal ratios LS_0/DR and SV/DR, respectively. Second, the MHS plots log $[\eta]$ versus log M_w of the branched polymer and its linear homolog are represented. Third, $g'(\log M_w)$ is estimated from the MHS plots. Fourth, $g(\log M_w)$ is estimated through Equation (3) with known value of ε; and finally $b_n(\log M_w)$ [or $b_w(\log M_w)$] are calculated from theoretical or semi-empirical relationships involving $g(b_n)$ [or $g(b_w)$]. These theoretical relationships are well-established for regular (star or comb) branched topologies, but have never been verified for randomly-branched topologies.[17] In what follows, only the case of randomly-branched topologies is considered.

For randomly-branched polymers characterized by Equation (8) and dissolved in a θ-solvent, Zimm and Stockmayer[9] developed the following approximate expressions for the geometric contraction factors. For trifunctional branch units and fixed molar masses, it is:

$$ g_3 = \left[\left(1 + \frac{b_n}{7}\right)^{1/2} + \frac{4 \, b_n}{9 \, \pi} \right]^{-1/2}; \quad (M_b = M_l) $$

(10)

For variations in both b and M, a weight-averaged g_3 is obtained through:

$$ \langle g_3 \rangle_w = \frac{6}{b_w} \left[\frac{1}{2} \left(\frac{2+b_w}{b_w}\right)^{1/2} \ln \left(\frac{(2+b_w)^{1/2} + b_w^{1/2}}{(2+b_w)^{1/2} - b_w^{1/2}}\right) - 1 \right] $$

(11)

For tetrafunctional branch units, the corresponding expressions are:

$$ g_4 = \left[\left(1 + \frac{b_n}{6}\right)^{1/2} + \frac{4 \, b_n}{3 \, \pi} \right]^{-1/2}; \quad (M_b = M_l) $$

(12)

$$ \langle g_4 \rangle_w = \frac{\ln[1 + b_w]}{b_w} $$

(13)

Even though originally developed for random polycondensations, Equation (10–13) have been extended onto radical polymerizations of bi- and multifunctional monomers of $f \geq 3$.[24] Furthermore, and in spite of large differences in their molecular distributions, Equation (10–13) are also normally applied onto polymers obtained by radical polymerization of bifunctional monomers with chain transfer to the polymer.[21,22,25–28]

For f-functional branched molecules with b branch units in θ-solvents, Kurata and Fukatsu[29] developed a model for a contraction factor that is analogous to g', but based on the ratio of Stokes radii. Some years later, and for a polymer with tetrafunctional branch units obtained by copolymerization of styrene and divinyl tetrachlorobenzene, Kurata et al.[30] suggested the value $\varepsilon = 0.6$. This value was adjusted after comparing theoretical predictions via Equation (2), (3), and (12) with intrinsic viscosity measurements of fractionated samples in a θ-solvent (cyclohexane at 35 °C).

SEC with triple detection is incapable of providing accurate estimates of $b_n(\log M)$ or $b_w(\log M)$; and the reasons for this are: (i) the Zimm–Stockmayer Equation (10–13) are only approximate, and assume θ-conditions; (ii) errors in required calculation parameters such as the MHS constants and the ε exponent of Equation (3); and (iii) biases in the determinations of $M_w(V)$ and $[\eta](V)$, caused by uncertainties in the interdetector volumes and by the low signal to noise ratios at the chromatogram tails.[31–33]

Several papers have investigated on the errors in the MMD when analyzing randomly-branched polymers by SEC. For a polymer characterized by Equation (8) with $f = 4$, Jackson[34] theoretically predicted only minor biases in the global dispersity $\bar{M}_z/\bar{M}_w$. For several chromatographically-complex polymers, Mourey et al.[35] suggested a method for estimating the Local Dispersity (LD) $M_w(V)/M_n(V)$ by triple detection combined with the universal calibration. For a mixture of linear and lightly branched polyesters, the LD is suggested to increase with the molar mass, but no LD values are presented.[35]

The articles by Gaborieau et al.,[6] Castignolles,[36] Castignolles et al.,[37], and Gaborieau and Castignolles,[38] have aimed at determining the LD of several branched

Randomly-Branched Polymers by Size Exclusion Chromatography with Triple Detection . . .

Macromolecular
Theory and Simulations

www.mts-journal.de

homopolymers synthesized by controlled radical polymerization with backbiting and chain transfer to the polymer. The LD was determined from independent estimates of $M_w(V)$ by LS_0/DR, and of $M_n(V)$ by SV/DR + universal calibration. In all cases, the LD was seen to increase with V, reaching a maximum of around 2 at the low molar mass limit of a poly(n-butyl acrylate).[6] In Castignolles,[36] the high LD observed at the low molar masses of a poly(n-hexyl acrylate) was suspect of being the result of artifacts in the data treatment. Possible causes of error are the low sensitivity of LS signals to low molar masses, and strong assumptions such as the θ-condition associated to the estimation of $M_n(V)$ by SV/DR + universal calibration.

The mentioned observations by Gaborieau et al.[6] are in contradiction with the very recent simulation results by Netopilík;[39] where the following assumptions were adopted: (i) the MMD responds to Equation (9) with the primary chains following the most probable distribution; and (ii) the logarithm of the chain-length of the linear molecules [log (N_0)] was considered a measure of elution volume. Many branched species of b branch units and N'_b total monomer units elute at the same elution volume as a linear chain of N_0 units, according to $N'_b = N_0/g_b$; where g_b is defined by Equation (1) and (12). The summation of the contributions of all N'_b (with $b = 0, 1, \ldots, 400$) enabled the calculation of the local chain-length distribution, and therefore the LD. Additionally, values of the ε exponent [Equation (3)] were estimated through a random-flight simulation (carried out in a cubic grid) of a model chain composed by 4 800 repeating units (b of them being tetrafunctional); on the basis of Monte-Carlo simulations with 20 000 independent molecular configurations and conformations at each value of b. The SEC model yielded almost indistinguishable values of g and g', and therefore $\varepsilon \approx 1$ was suggested. This observation is in accord with findings by Farmer et al.,[4] who claimed that either the radius of gyration or the viscosity radius can equivalently describe the SEC separation of molecules. The results by Netopilík[39] suggest that the LD decreases with V, attaining maximum values at the high-molar masses that range between 1.27 and 1.60. So far, no explanation can be given for the different tendencies and values of the LD observed by Netopilík[39] with respect to Gaborieau et al.[6] One important difference is that while the polymers analyzed by Gaborieau et al.[6] contained both long and short trifunctional branches, the polymer simulated by Netopilík[39] only contained long branches with tetrafunctional units.

The present computer simulation study was carried out under the auspices of the IUPAC project: "Data Treatment in SEC and Other Techniques of Polymer Characterization. Correction for Band Broadening and Other Sources of Error", Chair G. Meira, http://www.iupac.org/web/ins/2009-019-2-400. The first part of the work aims at elucidating the

mentioned controversy on the values and tendencies of the LD when randomly-branched polymers described by Equation (8) are analyzed by ideal SEC. The article also analyzes the errors introduced into the LCBD. In its second part of the work, the following additional sources of error are analyzed: presence of BB in the column, and contamination with random noise. All the computer work was carried out in Matlab.

2. Ideal Fractionation Model

An ideal SEC fractionation was simulated, in order to investigate the effects of the chromatographically-complex nature of random branched polymers. The following hypotheses are adopted: (i) representative calibrations of the branched classes are obtained from contraction factors calculated through the Zimm–Stockmayer equations; (ii) each molecular species in the distribution exhibits a fixed hydrodynamic volume that is independent of molecular configuration or conformation; and (iii) local dispersities are obtained from average properties calculated in small volumes that emulate a minor mixing in the detector cells.

Consider the simulated SEC analysis of a crosslinked polystyrene (obtained by copolymerization of styrene and divinylbenzene), and dissolved in a θ-solvent (cyclohexane at 34.5 °C). The weight-based distributions were calculated through Equation (9a) with $\overline{y}_w = 1250$ and $\gamma = 0.6$. The final values of $w_{b,l}$ were determined after normalizing the r.h.s. of Equation (9a) with the sum of the contributions by all the possible molecular species defined by (b, l). The upper limits of calculation were $l_{max} = 150\,000$ and $b_{max} = 75$. At such limits, the following negligible mass fractions were observed: 2.4×10^{-16} at l_{max}; and 1.3×10^{-6} for the branched class with $b_{max} = 75$. The weight MMDs of the total polymer and its branched classes are represented in Figure 1a. It should be noted that while continuous MMDs are represented, such distributions are strictly discrete. The following convention was adopted for the graphical representation of the continuous MMDs in Figure 1a: (i) the MMD of the total polymer is normalized to unitary area;[40] and (ii) for each of the branched classes, the area under their MMDs coincides with their mass fraction in the total distribution.

Table 1 presents the discrete number- and weight LCBDs [$N'(b)$ and $W'(b)$, respectively; with ($b = 0, 1, \ldots, 75$)]. These distributions were calculated through: $N'(b) = \sum_{l=1}^{150\,000}(w_{b,l}/M_{b,l})$ and $W'(b) = \sum_{l=1}^{150\,000} w_{b,l}$]. Table 1 also presents the number-average molar masses and dispersities of each branched class. As expected, the linear fraction (of $b = 0$) is the most abundant, and exhibits a global dispersity of almost 2. For increasing b's, the mass contributions are reduced, and the dispersities tend to
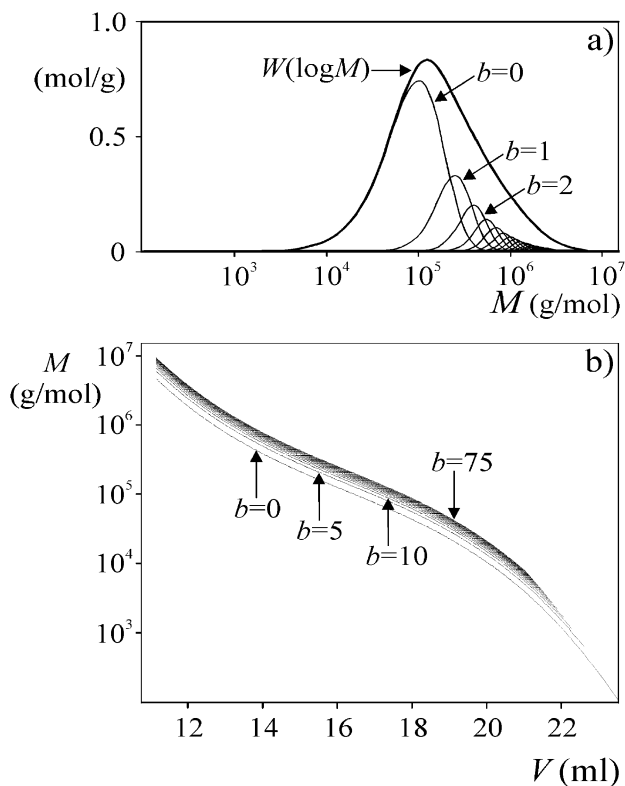
Figure 1. Basic simulation example: (a) continuous MMDs of the total polymer and branched classes of b (=0, 1, 2,..., 75) tetrafunctional branch units per molecule. (b) Molar mass calibrations of the linear fraction ($b=0$), and of the branched classes $b=5$, 10, ..., 75 (only a few calibrations are shown to avoid superimposition of curves).

Table 1. Basic simulation example. Number- and weight-based distributions of the number of long chain branches per molecule, and number-average molar masses and dispersities of the linear class ($b=0$), and branched classes with $b=1, 2, \ldots, 75$.

b	$N'(b)$	$W'(b)$	$\bar{M}_n(b)$	$\bar{M}_w(b)/\bar{M}_n(b)$
0	0.9051	0.5928	50 124	1.9979
1	0.0617	0.1616	200 392	1.2497
2	0.0168	0.0772	350 661	1.1427
3	0.0069	0.0451	500 929	1.0999
4	0.0034	0.0293	651 197	1.0768
5	0.0019	0.0204	801 466	1.0624
6	0.0012	0.0148	951,734	1.0525
7	0.0008	0.0111	1 102 003	1.0454
8	0.0005	0.0085	1 252 271	1.0399
9	0.0004	0.0067	1 402 540	1.0356
10	0.0003	0.0053	1 552 808	1.0322
⋮	⋮	⋮	⋮	⋮
75	9.089×10^{-9}	1.344×10^{-6}	11 320 255	1.0044

$$\log M_b(V) = \log M_l^\bullet(V) - \frac{1}{\alpha+1}\log g_4^\varepsilon(V);$$
$$(b = 1, 2, \ldots 75) \tag{16}$$

The following calibration was adopted for the linear class (curve $b=0$ of Figure 1b):

$$log\, M_l^\bullet(V) = -0.0036686 V^3 + 0.179044 V^2$$
$$- 3.13512 V + 24.4522 \tag{17}$$

Equation (17) corresponds to the chromatograms of a set of narrow polystyrene standards analyzed with a 2-column set (HRE4 and HRE5 from Waters), that covered a broad fractionation range. The following values were adopted for the MHS constants of linear polystyrene in cyclohexane at 34.5 °C: $k = 8.57 \times 10^{-4}$ dl g^{-1}; and $\alpha = 0.5$.[43]

The calibrations of branched classes with $b=1, 2, \ldots$ (Figure 1b), were calculated through Equation (16) after substituting Equation (17); with the parameters $\alpha = 0.5$ and $\varepsilon = 0.6$,[30] and the values of g_4 obtained from Equation (12) with $b = 1, 2, \ldots, 75$. Jackson[34] developed an expression that is equivalent to Equation (16), but assuming linear calibrations for the linear and branched classes.

Each i-th molecular species in the global MMD (with $i = 1, 2, \ldots, 150\,000 \times 76 = 11\,400\,000$), was characterized by the following variables: (i) the polymerization degrees (l_i, b_i); (ii) the molar mass $M_i = M_{b,l} = 104.15 \times l + 130.19 \times b$; (iii) the weight fraction $w_i = w_{b,l}$ [Equation (9a and b)]; (iv) the molar fraction $n_i = w_i/M_i$; (v) the contraction factors $g_{4,i}$ and $g'_{4,i}$ calculated through Equation (12) and (3) with

unity. The global averages are presented in the first row of Table 2; where the (number- and weight-based) average branching degrees were calculated through: $\bar{b}_n = \sum_b [N'(b) \times b]/\sum N'(b)$ and $\bar{b}_w = \sum_b [W'(b) \times b]/\sum W'(b)$.

Consider the equations employed for simulating the calibrations of the different branched classes. With perfect fractionation by hydrodynamic volume, one can write:

$$[\eta]_b(V) \times M_b(V) = [\eta]_l^\bullet(V) \times M_l^\bullet(V)$$
$$= \{K (M_l^\bullet)^{\alpha+1}\}(V); \quad (b = 1, 2, \ldots) \tag{14}$$

where $[\eta]_l^\bullet$ and $M_l^\bullet$ are the intrinsic viscosity and molar mass of the linear molecule that elutes at a given V. From Equation (2), (3), and (14), it results:[41,42]

$$g_4^\varepsilon = g'_4 = \frac{[\eta]_b(M_b)}{[\eta]_l(M_b)} = \frac{K(M_l^\bullet)^{\alpha+1}/M_b}{K(M_b)^\alpha} = \left(\frac{M_l^\bullet}{M_b}\right)^{\alpha+1} \tag{15}$$

Solving for M_b with the first and last terms of Equation (15), and then taking logarithms, one obtains:

www.MaterialsViews.com

Randomly-Branched Polymers by Size Exclusion Chromatography with Triple Detection . . .

Macromolecular
Theory and Simulations

www.mts-journal.de

Table 2. Basic simulation example: global average molar masses and branching degrees. The true values are highlighted in bold font.

	Source of bias	Estimated distributions	$\bar{M}_n$	$\bar{M}_w$	$\bar{M}_w/\bar{M}_n$	$\bar{b}_n$	$\bar{b}_w$	$\bar{b}_w/\bar{b}_n$
"True" averages	−	−	76 536	323 420	4.2257	0.1758	1.4858	8.4516
Ideal Fractionation	(1)	$W(\log M_n)$	76 536	322 650	4.2157	−	−	
Model	(1)	$W(\log M_w)$	76 590	323 420	4.2228	−	−	
	(1)	$W(b_n)$	−	−	−	0.1754	1.4549	8.2947
Estimates from simulated	(1) + (2) + (3)	$\hat{W}^{BB}(\log \hat{M}_w^{BB})$ and $\hat{W}^{BB}(\hat{b}_n^{BB})$	124 130[a]	348 920[a]	2.8110[a]	0.3505[a]	1.6213[a]	4.7257
chromatograms	(1) + (2)	$\hat{W}^{BB}(\log \hat{M}_w^{BB})$ and $\hat{W}^{BB}(\hat{b}_n^{BB})$	81 177	323 420	3.9842	0.2340	1.4917	6.3748

(1) Ideal fractionation by hydrodynamic volume with a minor mixing in the detection cells. (2) BB-affected chromatograms. (3) Contamination of chromatograms with additive random noise. [a]Calculation restricted to the Calculation Range (Figure 3).

$b_n = b = 0, 1, 2, \ldots, 75$; (vi) the elution volume V_i through Equation (16) and (17); and (vii) the intrinsic viscosity $[\eta]_i = g'_{4,i} K M_i^\alpha$ [Equation (2)]. Then, all 11 400 000 molecular species were reordered according to increasing elution volumes (V_i). A truly perfect fractionation by hydrodynamic volume would produce a discontinuous mass chromatogram represented by a train of impulses, with an impulse at each discrete V_i. To simulate a more realistic (albeit still ideal) mass chromatogram, a minor mixing was simulated in the detection cells, while still assuming perfect fractionation in the columns. Such minor mixing was simulated by first dividing the total range of elution volumes into 171 regular intervals of $\Delta V = 75$ µl (a volume equal to one half the added volumes of the 3 typical detectors in triple detection); and then calculating the following instantaneous averages at each discrete V_j ($j = 1, \ldots, 171$): (i) weight-fraction $W(V_j) = \sum_i w_i$; (ii) average molar masses $M_n(V_j)$ [$= \sum_i n_i M_i / \sum_i n_i$] and $M_w(V_j)$ [$= \sum_i w_i M_i / \sum_i w_i$]; (iii) weight-average intrinsic viscosity $[\eta]_w(V_j)$ [$= \sum_i w_i [\eta]_i / \sum_i w_i$]; (iv) average branching degrees [$b_n(V_j) = \sum_i n_i b_i / \sum_i n_i$ and $b_w(V_j) = \sum_i w_i b_i / \sum_i w_i$]; and (v) weight-average contraction factor $g_{4,w}(V_j) = \sum_i w_i g_{4,i} / \sum_i w_i$. All the previous summations are extended over all i species contained in each j-th interval. The logarithmic nature of the calibration curve induces a large variation in the number of molecular species (i) contained in each successive interval. Thus, while the first three intervals (with $j = 1, 2, 3$), respectively contain 880 841, 788 179, and 706 328 types of molecular species; the last 11 intervals (of $j = 161, 162, \ldots, 171$), respectively contain 2, 1, 2, 1, 0, 2, 0, 0, 0, 0, and 1 molecular types. The low number of molecular types (and even absence of molecules) in the final elution volume intervals is a consequence of the high resolution of SEC at such limit. In what follows, we adopt for simplicity: $V_j \equiv V$. The final results are in Figure 2 and in the mid-section of Table 2. Additionally, Sections 1 and 2 of the Supplementary Information present a calculation flow-sheet and some of the intermediate simulation variables.

Figure 2a shows the almost-coincident local calibrations $\log M_w(V)$ and $\log M_n(V)$. At the lower molar masses, these calibrations are also almost coincident with the calibration of the linear class; while at the higher molar masses tend toward the calibration of the highest branched class. Figure 2b presents the LDs based on the average molar masses [$M_w(V)/M_n(V)$] and on the average branching degrees [$b_w(V)/b_n(V)$]. While $M_w(V)/M_n(V)$ exhibits a moderate maximum of 1.0035 at $M = 386 000$ g mol^{-1}; $b_w(V)/b_n(V)$ monotonically increases with V, and tends to 1.1 at high V's (where $b_w(V) \approx b_n(V) \approx 0$, and most of the molecules are linear). Note that the contribution of linear molecules towards $b_w(V)$ and $b_n(V)$ is indirect, through the denominators of $\sum_i n_i b_i / \sum_i n_i$ and $\sum_i w_i b_i / \sum_i w_i$. The final oscillations in $M_w(V)/M_n(V)$ and $b_w(V)/b_n(V)$ at high V's are caused by the few molecular species and/or absence of molecules in the final ΔV intervals.

Figure 2c shows that the true unbiased MMD [$W(\log M)$] almost coincides with its estimates $W(\log M_n)$ and $W(\log M_w)$; that were respectively obtained from [$W(V)$, $M_n(V)$] and [$W(V)$, $M_w(V)$]. As expected, $W(\log M_n)$ produces an unbiased global $\bar{M}_n$, but slightly underestimated values of $\bar{M}_w$ and $\bar{M}_w/\bar{M}_n$; while $W(\log M_w)$ produces an unbiased global $\bar{M}_w$, but an overestimated $\bar{M}_n$ and an underestimated $\bar{M}_w/\bar{M}_n$ (Table 2).

Figure 2d compares the true discrete weight LCBD [$W'(b)$] with its estimate $W(b_n)$, obtained from $W(V)$ and $b_n(V)$. Following the case of continuous MMDs, continuous LCBDs were also normalized to unitary area. The branching function $b_n(\log M_w)$ was obtained from $b_n(V)$ and $\log M_w(V)$, and the global averages $\bar{b}_n$ and $\bar{b}_w$ (see Table 2) were calculated through: $\bar{b}_n = \sum [[W(\log M_w)/M_w] \times b_n(\log M_w)] / \sum [W(\log M_w)/M_w]$ and $\bar{b}_w = \sum [W(\log M_w) \times$
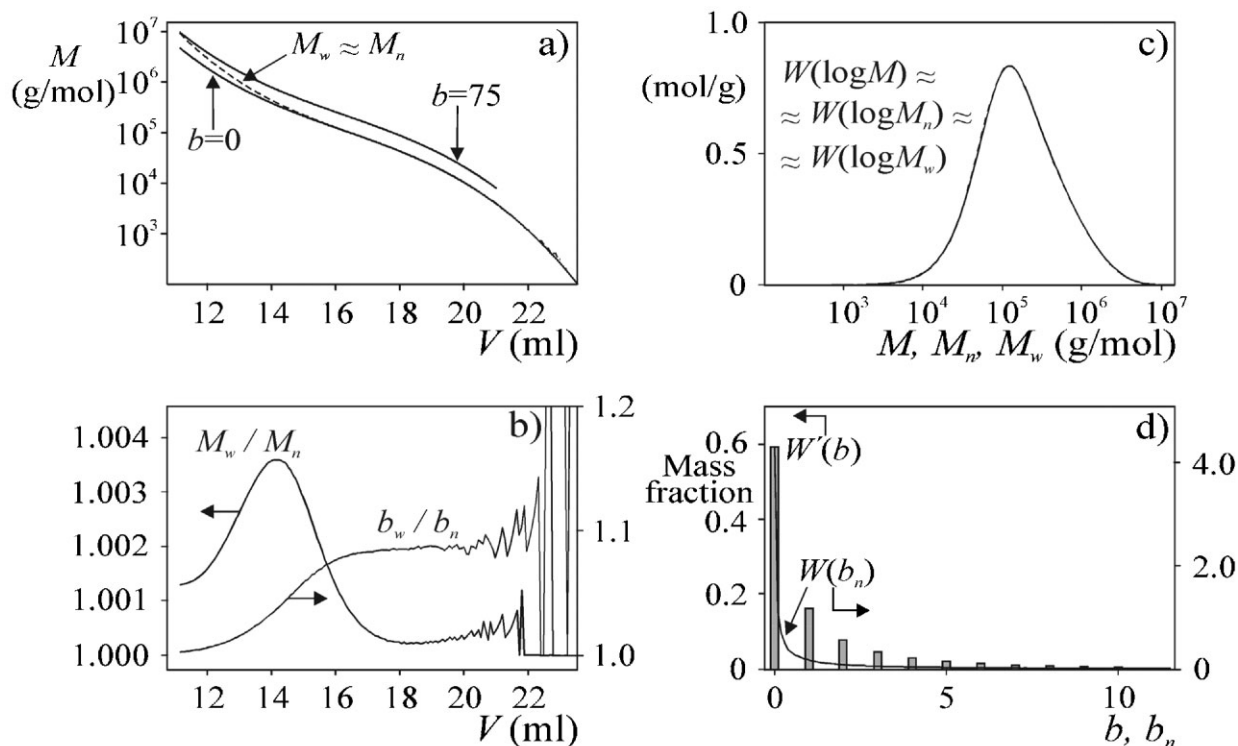
Materials
Views

www.MaterialsViews.com

Macromol. Theory Simul. **2014,** *23,* 90–100
© 2013 WILEY-VCH Verlag GmbH Co. KGaA, Weinheim

Macromolecular
Journals

95

Figure 2. Basic example and ideal SEC. (a) Local (or "ad hoc") molar mass calibrations. (b) Local dispersities $M_w(V)/M_n(V)$ and $b_w(V)/b_n(V)$. (c) True MMD [$W(\log M)$], and its estimates $W(\log M_n)$ and $W(\log M_w)$. (d) True discrete weight LCBD [$W'(b)$], and its continuous estimate [$W(b_n)$].

$b_n(\log M_w)]/\sum W(\log M_w)$. While the estimate of $\overline{b}_n$ (= 0.1754) almost coincides with the true value of 0.1758, a larger difference is observed between the estimate of $\overline{b}_w$ (= 1.4549) and the true value (= 1.4858).

3. Effects of Band Broadening and Measurement Noise

Let us represent the ideal DR, LS_0, and SV chromatograms by $s_{DR}(V)$, $s_{LS}(V)$, and $s_{SV}(V)$, respectively. Such ideal chromatograms (i.e.: BB-free, noise-free, and perfectly corrected for interdetector volumes) were calculated through:

$$s_{DR}(V) = k_{DR}W(V); \quad \text{with} \quad k_{DR} = 1 \tag{18}$$

$$s_{LS}(V) = k_{LS}W(V)M_w(V); \quad \text{with} \quad k_{LS} = 1.5 \times 10^{-6} \tag{19}$$

$$s_{SV}(V) = k_{SV}W(V)[\eta]_w(V); \quad \text{with} \quad k_{SV} = 0.01 \tag{20}$$

where the factors k_{DR}, k_{LS}, and k_{SV} are assumed constant (an assumption that is inapplicable onto oligomers or copolymers exhibiting variation of $\partial n/\partial c$ with V). Note that these factors also include the detector gains and

physical parameters specific to the corresponding detection system. Furthermore, the values of k_{DR}, k_{LS}, and k_{SV} were selected in order to produce similar numerical values of the simulated ideal chromatograms $s_{DR}(V)$, $s_{LS}(V)$, and $s_{SV}(V)$ (Figure 3a).

The uniform BB function in columns and capillaries is represented by $h(V)$ [see Figure 3a], and it was obtained from the mass chromatogram of a pure solvent injected in the above-mentioned experimental system. The BB-affected chromatograms $s_{DR}^{BB}(V), s_{LS}^{BB}(V)$, and $s_{SV}^{BB}(V)$ were obtained by convolution of $h(V)$ with $s_{DR}(V)$, $s_{LS}(V)$, and $s_{SV}(V)$, respectively. Then, such chromatograms were contaminated with zero-mean white noises through:

$$\tilde{s}_d^{BB}(V) = s_d^{BB}(V) + \xi_d(V); \quad (d = DR, LS, SV) \tag{21}$$

where the oversymbol "~" indicates a noise-affected variable; $\tilde{s}_d^{BB}(V)$ is any generic BB-affected and noisy chromatogram; and $\xi_d(V)$ is a Gaussian random sequence of zero mean and constant standard deviation σ_d. For the LS_0 chromatogram, σ_d was adopted equal to 0.5% of the maximum. For the DR and SV chromatograms, $\sigma_d = 0.1\%$ of their maximum values. Figure 3a compares the BB-affected and noisy chromatograms with their ideal counterparts. Note the small effect of BB, due to the fact that the mass chromatogram (of $\overline{M}_w/\overline{M}_n = 4.2257$) is much broader than

www.MaterialsViews.com

Randomly-Branched Polymers by Size Exclusion Chromatography with Triple Detection . . .

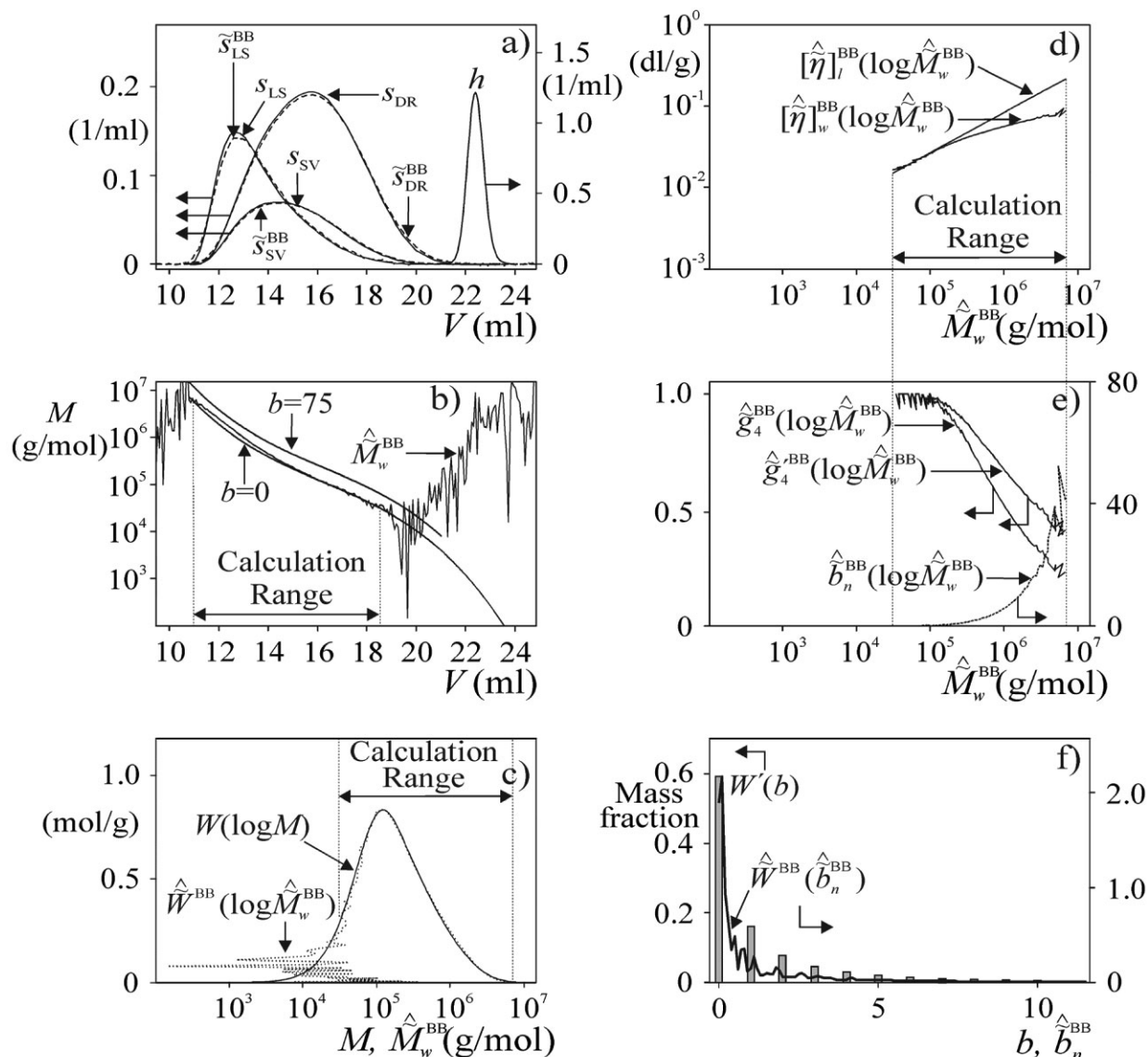Macromolecular
Theory and Simulations

www.mts-journal.de

Figure 3. Basic example with BB and measurement noise. (a) Ideal chromatograms, noisy and BB-affected chromatograms, and BB function $h(V)$. (b) Local calibration, and limiting noise-free calibrations with $b = 0$ and $b = 75$. (c) True and estimated MMDs. (d) MHS plots of the analyzed polymer and its linear homolog inside the Calculation Range. (e) Estimated contraction factors and resulting branching function. (f) True and estimated LCBDs.

the BB function $h(V)$. Also note that (due to the relatively low adopted standard deviations) the noisy chromatograms look all quite smooth [except perhaps for minor oscillations that are visible in $\tilde{s}_{LS}^{BB}(V)$].

In all that follows, the oversymbol "$\hat{}$" indicates that the variable was calculated from the BB-affected and noisy chromatograms. From Equation (18) and (19), the local calibration of Figure 3b was calculated through:

$$\log \hat{\tilde{M}}_w^{BB}(V) = \log \left(\frac{k_{DR}}{k_{LS}} \frac{\tilde{s}_{LS}^{BB}(V)}{\tilde{s}_{DR}^{BB}(V)} \right) \qquad (22)$$

This calibration is highly oscillatory outside the Calculation Range (Figure 3b). Figure 3c compares the true continuous MMD [$W(\log M)$] with its estimate $\hat{\tilde{W}}(\log \hat{\tilde{M}}_w^{BB})$ obtained from $\tilde{s}_{DR}^{BB}(V)$ and $\log \hat{\tilde{M}}_w^{BB}(V)$. While $\log \hat{\tilde{M}}_w^{BB}(V)$ appropriately reproduces the high molar mass half of the MMD, it is unacceptably noisy in its low molar mass half, due to the poor signal-to-noise ratio of $\tilde{s}_{LS}^{BB}(V)/\tilde{s}_{DR}^{BB}(V)$ in Equation (22). To solve for this problem, it has been suggested to extrapolate the local calibration outside the Calculation Range.[33,44]

Materials
Views

www.MaterialsViews.com

Macromol. Theory Simul. **2014**, *23*, 90–100

© 2013 WILEY-VCH Verlag GmbH Co. KGaA, Weinheim

Macromolecular
Journals

97

Consider the estimation of the branching function and continuous LCBD inside the feasible Calculation Range of Figure 3d and e. First, from Equation (18) and (20), the intrinsic viscosity of the branched polymer was calculated through:

$$[\hat{\eta}]_w^{BB}(V) = \frac{k_{DR}\,\tilde{s}_{SV}^{BB}(V)}{k_{SV}\,\tilde{s}_{DR}^{BB}(V)} \qquad (23)$$

and the MHS plot $log[\hat{\eta}]_w^{BB}(log\,\hat{\bar{M}}_w^{BB})$ was obtained from $[\hat{\eta}]_w^{BB}(V)$ and $log\,\hat{\bar{M}}_w^{BB}(V)$ (Figure 3d). Similarly, the MHS plot of the linear homolog $log\,[\hat{\eta}]_l^{BB}(log\,\hat{\bar{M}}_w^{BB})$ was obtained from $[\hat{\eta}]_l^{BB}(V)\left[= K \times \hat{\bar{M}}_w^{BB}(V)^\alpha\right]$ and $log\,\hat{\bar{M}}_w^{BB}(V)$ (Figure 3d). As expected, both MHS plots coincide at the low molar masses, where the molecules are essentially linear. Second, $\hat{g}'^{BB}_4(log\,\hat{\bar{M}}_w^{BB})$ was obtained through (see Figure 3e):

$$\hat{g}'^{BB}_4(log\,\hat{\bar{M}}_w^{BB}) = \frac{[\hat{\eta}]_w^{BB}(log\,\hat{\bar{M}}_w^{BB})}{[\hat{\eta}]_l^{BB}(log\,\hat{\bar{M}}_w^{BB})} \qquad (24)$$

Third, $\hat{g}_4^{BB}(log\,\hat{\bar{M}}_w^{BB})$ was calculated from $\hat{g}'^{BB}_4(log\,\hat{\bar{M}}_w^{BB})$ and Equation (3) with $\varepsilon = 0.6$ (Figure 3e). Fourth, the branching function estimate $\hat{\bar{b}}_n^{BB}(log\,\hat{\bar{M}}_w^{BB})$ was obtained by injecting the values of $\hat{g}_4^{BB}(log\,\hat{\bar{M}}_w^{BB})$ into Equation (12) (Figure 3e). Finally, the LCBD estimate $\hat{\bar{W}}^{BB}(\hat{\bar{b}}_n^{BB})$ was obtained from $\hat{\bar{W}}^{BB}(log\,\hat{\bar{M}}_w^{BB})$ and $\hat{\bar{b}}_n^{BB}(log\,\hat{\bar{M}}_w^{BB})$ (Figure 3f).

The global averages were evaluated in the Calculation Range of Figure 3c–e, and are presented in the penultimate row of Table 2. The following expressions were employed for calculating the average branching degrees:
$$\hat{\bar{\bar{b}}}_n = \sum\left[\left[\hat{\bar{W}}^{*BB}(log\,\hat{\bar{M}}_w^{BB})/\hat{\bar{M}}_w^{BB}\right] \times \hat{\bar{b}}_n^{BB}(log\,\hat{\bar{M}}_w^{BB})\right]\bigg/\sum\left[\hat{\bar{W}}^{BB}(log\,\hat{\bar{M}}_w^{BB})/\hat{\bar{M}}_w^{BB}\right]$$
and $\quad\hat{\bar{\bar{b}}}_w = \sum\left[\hat{\bar{W}}^{*BB}(log\,\hat{\bar{M}}_w^{BB}) \times \hat{\bar{b}}_n^{BB}(log\,\hat{\bar{M}}_w^{BB})\right]\bigg/\sum\hat{\bar{W}}^{BB}(log\,\hat{\bar{M}}_w^{BB}).$ As expected, all the global averages appear overestimated because the molecular species with $M < 32\,800\,\mathrm{g\,mol^{-1}}$ were excluded from the calculations. For completeness, the last row of Table 2 presents the average values obtained from the BB-affected but noise-free chromatograms, and calculated in the complete range of the chromatograms. As expected, the estimates of $\overline{M}_w$ and $\overline{b}_w$ are unbiased, while $\overline{M}_n$ and $\overline{b}_n$ are overestimated, and therefore $\overline{M}_w/\overline{M}_n$ and $\overline{b}_w/\overline{b}_n$ are underestimated (last row of Table 2).

4. Further Simulation Results

4.1. Effect of Variations in the Elution Volume Interval

The basic simulation example was reconsidered, to analyze the effects of variations in the averaging interval ΔV

(initially adopted $= 75\,\mu L$). To highlight the effect of the chromatographically-complex nature of the polymer, ΔV should be small enough to emulate a perfect fractionation by hydrodynamic volume, but also large enough to allow for a minor mixing in the detector cells (in the limit of $\Delta V \to 0$, the mass chromatogram is a train of impulses). The following alternative ΔV values were investigated: 10, 25, and 150 μL. Figure 4 presents the effects on the LD functions. When ΔV is reduced to 25 or 10 μL, all the $M_w(V)/M_n(V)$ function is slightly lowered: while a significant increase in $M_w(V)/M_n(V)$ is observed when ΔV is doubled to 150 μl (Figure 4a). In contrast, variations of ΔV show a negligible effect on $b_w(V)/b_n(V)$ (Figure 4b).

4.2. Sensitivity to Variations in ε, k, and α

Consider the effect of errors in the parameters (ε, k, and α), when employed to calculate the global averages $\overline{b}_n$ and $\overline{b}_w$ from the ideal (BB-free and noise-free) chromatograms. The averages proved moderately sensitive to errors in ε; and for example a variation of $+10\%$ in ε induced reductions of 13% in $\overline{b}_n$ and 16% in $\overline{b}_w$. In contrast, small errors in k or α importantly affect the same estimates. Thus, variations of $+1\%$ in k, induced variations of $+8\%$ in $\overline{b}_w$ and $+43\%$ in $\overline{b}_n$; while variations of $+1\%$ in α induced variations of $+58\%$ in $\overline{b}_w$ and $+250\%$ in $\overline{b}_n$.
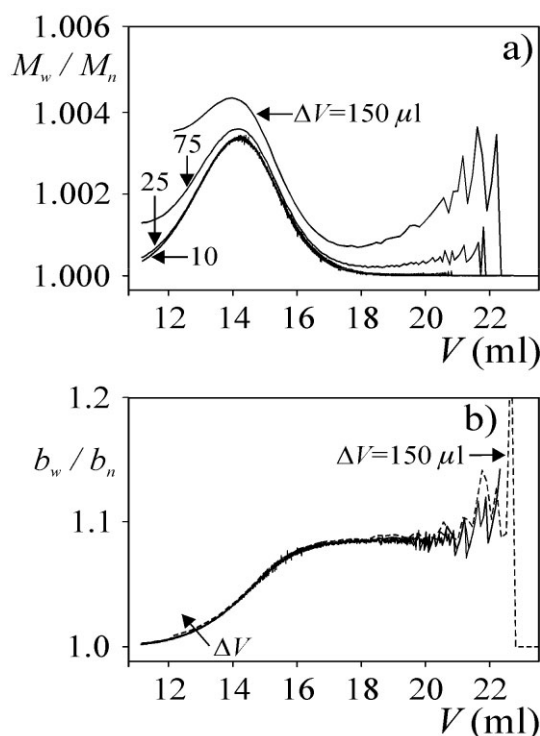

Figure 4. Sensitivity of LDs toward changes in the mixing interval ΔV with respect to the basic case of 75 μL. (a) Effect on $M_w(V)/M_n(V)$. (b) Effect on $b_w(V)/b_n(V)$.

www.MaterialsViews.com

Randomly-Branched Polymers by Size Exclusion Chromatography with Triple Detection . . .

Macromolecular
Theory and Simulations

www.mts-journal.de

Table 3. Simulation example of an equivalent branched polymer containing trifunctional branch units: global average molar masses and branching degrees. The true values are highlighted in bold font.

	Source of bias	Estimated distributions	M_n	M_w	M_w/M_n	b_n	b_w	b_w/b_n
"True" averages	–	–	**72 315**	**185 690**	**2.5678**	**0.2222**	**0.8556**	**3.8505**
Estimates from simulated chromatograms	$(1)+(2)+(3)$	$\hat{W}^{BB}(log\,\hat{M}_w^{BB})$ and $\hat{W}^{BB}(\hat{b}_n^{BB})$	122 010[a]	203 850[a]	1.6708[a]	0.4155[a]	0.8832[a]	2.1256[a]

(1) Ideal fractionation by hydrodynamic volume with a minor mixing in the detection cells. (2) BB-affected chromatograms. (3) Contamination of chromatograms with additive random noise. [a]Calculation restricted to a feasible Calculation Range (see Figure S3c in the Supplementary Information).

4.3. Polymer with Trifunctional Branch Units

To investigate the effect of functionality of branch units, the basic example was re-simulated, but for a polymer containing trifunctional units; and defined by Equation (8) with $p = 0.9984$ and $\rho = 0.00048$. The global averages are shown in the first row of Table 3. Compared to the tetrafunctional case (Table 2), the trifunctional polymer exhibits similar values of $\overline{M}_n$ and $\overline{b}_n$, but considerably reduced global dispersities (Table 3). To simulate the SEC fractionation, the calibrations of the branched classes were recalculated through Equation (16) and (17), but introducing the g_3 contraction factors calculated through Equation (10), while maintaining all other parameters unchanged. The estimated global averages exhibit very similar tendencies to the tetrafunctional case (Table 3). For completeness, Section S3 of the Supplementary Information presents the basic MMDs and the evolution of the main output variables.

5. Conclusion

The simulated examples assumed θ-condition, while good solvents are employed in real SEC. So far, it is impossible to produce representative predictions for an equivalent SEC fractionation in a good solvent. The reasons are experimental and theoretical limitations on the effect of good solvents on: (i) the g and g' contraction factors, and (ii) the distribution of column pores. For the best known case of star polymers, direct determinations of the g and g' contraction factors indicate a relatively minor effect of solvent power on the draining exponent ε.[17] If this were also the case of randomly-branched polymers, then the main observations presented in this work would be applicable to the case of good solvents.

Following Netopilík,[39] the developed SEC model considers a random polymer with tetrafunctional branch units dissolved in a θ-solvent, and under perfect fractionation by hydrodynamic volume. However, different (but complementary) theoretical models were employed for estimating the molar mass based LD. In this work, nonlinear molar mass calibrations were assumed, and $M_w(V)/M_n(V)$ is the result of a minor mixing in the detector cells. In Netopilík,[39] linear calibrations were assumed, and $M_w(V)/M_n(V)$ was estimated from readjusted contraction factors obtained by Monte-Carlo simulations involving a variety of molecular configurations and conformations. In spite of the different approaches, the results by Netopilík[39] are qualitatively similar to those of the present work in that $M_w(V)/M_n(V)$ tends to unity at the low molar masses, and attains a maximum at a high molar mass value. However, our prediction for the maximum of $M_w(V)/M_n(V)$ ($=1.0035$) is considerably lower than the values predicted by Netopilík.[39] The qualitative tendencies of $M_w(V)/M_n(V)$ calculated in this work coincide with Netopilík,[39] but differ substantially from those of Gaborieau et al.,[6] where the LD was seen to increase (rather than decrease) with elution volume. The reasons for these discrepancies remain unknown, and more accurate experimental measurements are required to elucidate the controversy.

Unlike previous theoretical investigations,[34,39] the present work also analyzed the errors in the LCBD, and the effects of BB and measurement noise. For perfectly accurate and noise-free measurements, BB alone induces a negligible biases into the global averages (bottom row of Table 2); and this result seems reasonable bearing in mind the broad MMDs of randomly-branched polymers. In contrast, the effect of measurement noise is serious, and possibly a main limitation of triple detection SEC. In effect, even minor noises induce intolerable errors in the estimates of $M_w(V)$ and $[\eta]_w(V)$ at the chromatogram tails, thus preventing quantitative estimations of the MMD and LCBD outside the feasible calculation range. Furthermore, the branching function and LCBD are highly

sensitive toward errors in the MHS parameters. Curiously however, errors in the ε exponent proved relatively less important; and this result is consistent with the observation by Netopilík[39] on the minor effect of the ε exponent on the SEC fractionation mechanism.

In summary, the main result of this article is that under ideal conditions, the chromatographically complex nature of random-branched polymers does not prevent the accurate determination of the MMD, and (to a lesser degree) of the LCBD. On the negative side, the highly nonlinear nature of the required data processing renders such determinations extremely sensitive to measurement noise and to errors in the calculation parameters.

[1] I. Vittorias, M. Parkinson, K. Klimke, B. Debbaut, M. Wilhelm, *Rheol. Acta* **2007**, *46*, 321.

[2] J. Lesec, M. Millequant, *Int. J. Polym. Anal. Charact.* **1996**, *2*, 305.

[3] Y. Brun, *J. Chromat. Relat. Techn.* **1998**, *21*, 1979.

[4] B. S. Farmer, K. Terao, J. W. Mays, *Int. J. Polym. Anal. Charact.* **2006**, *11*, 3.

[5] M. Gaborieau, R. G. Gilbert, A. Gray-Weale, J. M. Hernandez, P. Castignolles, *Macromol. Theor. Simul.* **2007**, *16*, 13.

[6] M. Gaborieau, J. Nicolas, M. Save, B. Charleux, J.-P. Vairon, R. G. Gilbert, P. Castignolles, *J. Chromatogr. A.* **2008**, *1190*, 215.

[7] S. Greene, in *Encyclopedia of Chromatography* (Ed: J. Cazes), Marcel Dekker, Inc., New York, USA **2001**, p. 738.

[8] S. Podzimek, *Light Scattering, Size Exclusion Chromatography and Asymmetric Flow Field Flow Fractionation: Powerful Tools for the Characterization of Polymers, Proteins and Nano-particles*, J. Wiley & Sons, Inc., Hoboken, NJ, USA **2011**.

[9] B. H. Zimm, W. H. Stockmayer, *J. Chem. Phys.* **1949**, *17*, 1301.

[10] W. H. Stockmayer, M. Fixman, *Ann. NY Acad. Sci.* **1953**, *57*, 334.

[11] B. H. Zimm, R. W. Kilb, *J. Polym. Sci.* **1959**, *37*, 19.

[12] G. C. Berry, *J. Polym. Sci. A-2.* **1971**, *9*, 687.

[13] J. Roovers, in *Encyclopedia of Polymer Science and Engineering*. (Ed: J. I. Kroschwitz), 2nd ed. Wiley-Interscience, New York **1985**, p. 478.

[14] P. Tackx, J. Tacx, *Polymer* **1998**, *39*, 3109.

[15] A. M. Striegel, W. W. Yau, J. J. Kirkland, D. D. Bly, *Modern Size-Exclusion Liquid Chromatography. Practice of Gel Permeation and Gel Filtration Chromatography*. 2nd ed., J. Wiley & Sons, Hoboken, NJ, USA **2009**.

[16] P. J. Flory, T. G. Fox, *J. Am. Chem. Soc.* **1951**, *73*, 1904.

[17] W. Burchard, *Adv. Polym. Sci.* **1999**, *143*, 113.

[18] W. H. Stockmayer, *J. Chem. Phys.* **1943**, *11*, 45.

[19] P. J. Flory, *Chem Rev.* **1946**, *39*, 137.

[20] C. D. Thurmond, B. H. Zimm, *J. Polym. Sci.* **1952**, *8*, 477.

[21] J. R. Vega, D. A. Estenoz, H. M. Oliva, G. R. Meira, *Int. J. Polym. Anal. Charact.* **2001**, *6*, 339.

[22] R. J. Minari, V. I. Rodriguez, D. A. Estenoz, J. R. Vega, G. R. Meira, L. M. Gugliotta, *J. Appl. Polym. Sci.* **2010**, *116*, 590.

[23] S. Ahn, H. Lee, S. Lee, T. Chang, *Macromolecules* **2012**, *45*, 3550.

[24] P. J. Flory, *J. Chem. Phys.* **1949**, *17*, 303.

[25] G. R. Meira, J. R. Vega, M. M. Yossen, in *Ewing's Analytical Instrumentation Handbook*. (Ed: J. Cazes), 3rd ed. Marcel Dekker, Inc., New York, USA **2004**, p. 825.

[26] S. Grcev, P. Schoenmakers, P. Iedema, *Polymer* **2004**, *45*, 39.

[27] C. Kim, J. Sainte Beuve, S. Guilbert, F. Bonfils, *Eur. Polym. J.* **2009**, *45*, 2249.

[28] Y. Yu, P. J. DesLauriers, D. C. Rohlfing, *Polymer* **2005**, *46*, 5165.

[29] M. Kurata, M. Fukatsu, *J. Chem. Phys.* **1964**, *41*, 2934.

[30] M. Kurata, M. Abe, M. Iwama, M. Matsushima, *Polym. J.* **1972**, *3*, 729.

[31] O. Procházka, P. Kratochvíl, *J. Appl. Polym. Sci.* **1986**, *31*, 919.

[32] R. Lew, P. Cheung, S. Balke, T. Mourey, *J. Appl. Polym. Sci.* **1993**, *47*, 1685.

[33] J. R. Vega, G. R. Meira, *J. Liq. Chrom. Rel. Technol.* **2001**, *24*, 901.

[34] C. Jackson, *J. Chromatogr. A* **1994**, *662*, 1.

[35] T. H. Mourey, K. A. Vu, S. T. Balke, in *ACS Symp. Ser.* (Ed: T. Provder), Washington, USA **1999**, p. 20.

[36] P. Castignolles, *Macromol. Rapid Commun.* **2009**, *30*, 1995.

[37] P. Castignolles, R. Graf, M. Parkinson, M. Wilhelm, M. Gaborieau, *Polymer* **2009**, *50*, 2373.

[38] M. Gaborieau, P. Castignolles, *Anal. Bioanal. Chem.* **2009**, *399*, 1413.

[39] M. Netopilík, *J. Chromatogr. A* **2012**, *1260*, 97.

[40] D. W. Shortt, *J. Liq. Chromatogr.* **1993**, *16*, 3371.

[41] W. S. Park, W. W. Graessly, *J. Polym. Sci. Phys. Ed.* **1977**, *15*, 85.

[42] G. R. Meira, in *Modern Methods of Polymer Characterization*. (Eds: H. G. Barth, J. W. Mays), J. Wiley & Sons, Inc., New York, USA **1991**, p. 67.

[43] H. L. Wagner, *J. Phys. Chem. Ref. Data* **1985**, *14*, 1101.

[44] Y. Brun, M. Gorenstein, N. Hay, *J. Liq. Chromatogr. Relat. Technol.* **2000**, *23*, 2615.